

# SOME ASPECTS OF NEUTRON-CAPTURE GAMMA RAYS\*

Lowell M. Bollinger

## I. OUTLINE OF THE FIELD

Experiments with neutron-capture  $\gamma$  rays may be divided into three categories — those concerned with the mechanisms of the  $(n, \gamma)$  reaction, those that make use of  $(n, \gamma)$  transitions to study the characteristics of low-energy nuclear states, and a variety of others. In this review we will attempt to survey briefly the status of technical developments, to give some examples of the kinds of physical questions that are studied, and to make some remarks about the prospects for the future. However, this is not intended to be a complete or a balanced review. In order to make the paper comprehensible and hopefully interesting to the many in the audience who are not nuclear physicists, we will omit many topics altogether and illustrate others only by means of the results obtained in the average-resonance-capture measurements carried out recently at Argonne. A very detailed description of the whole subject of neutron-capture  $\gamma$  rays is provided by the Proceedings [1] of the International Symposium on Neutron Capture Gamma-Ray Spectroscopy, Studsvik, 1969.

For the benefit of those of you who are not involved in the study of neutron-capture  $\gamma$  rays, let us start by briefly considering several basic questions: What are neutron-capture  $\gamma$  rays, how are they studied, and why are they interesting? Figure 1 attempts to answer the first of these. When a neutron is captured in a nucleus, an initial state is formed with an excitation energy equal to the neutron-binding energy plus the energy of the incident neutron. This excitation energy (typically 8 MeV) may be carried off by a radiative transition to a nuclear state at lower energies. Since hundreds of thousands of such states are available in most heavy nuclides, the spectrum of capture  $\gamma$  rays is very complex. The spectrum may be thought of as consisting of three parts: (1) the resolved high-energy lines formed by transitions directly from the initial state to low-energy final states, (2) the resolved low-energy lines formed by transitions between the low-energy states, and (3) the unresolved mass of lines at intermediate energy. In this review we will be concerned primarily with the resolved high-energy and low-energy lines because these are the parts of the spectrum that are well enough understood to provide most of the information of physical interest.

The second question is "How are the neutron-capture  $\gamma$ -ray spectra measured?" A complete answer would be very long, of course, but the main truth is summarized in Fig. 2. Briefly, Ge(Li) detectors are used for the full energy range (0-10 MeV) and, when an intense source is available, high-resolution diffraction spectrometers are used for the low-energy end of the spectrum. Also, internal-conversion spectrometers are playing an increasingly useful role.

The question "What neutron sources are used?" is answered by Fig. 3. This figure is a qualitative representation of how the counting rate for a typical nucleus varies when measured with a time-of-flight neutron spectrometer. The classes of neutron sources that are used in most studies of neutron-capture  $\gamma$  rays are indicated on the figure. On the left are the thermal neutrons provided by reactors. A basic feature of such a source is that the state formed by neutron capture is at an arbitrary, unchangeable energy

\* Work performed under the auspices of the U.S. Atomic Energy Commission. Prepared for the International Meeting on Perspectives of Neutron Spectroscopy, Dubna (USSR) October 13-16, 1970.

Argonne National Laboratory, Argonne, Illinois, USA. Published in Problemy Fiziki Élementarnykh Chastits i Atomnogo Yadra, Vol. 2, No. 4, pp. 885-916, 1972.

© 1973 Consultants Bureau, a division of Plenum Publishing Corporation, 227 West 17th Street, New York, N. Y. 10011. All rights reserved. This article cannot be reproduced for any purpose whatsoever without permission of the publisher. A copy of this article is available from the publisher for \$15.00.

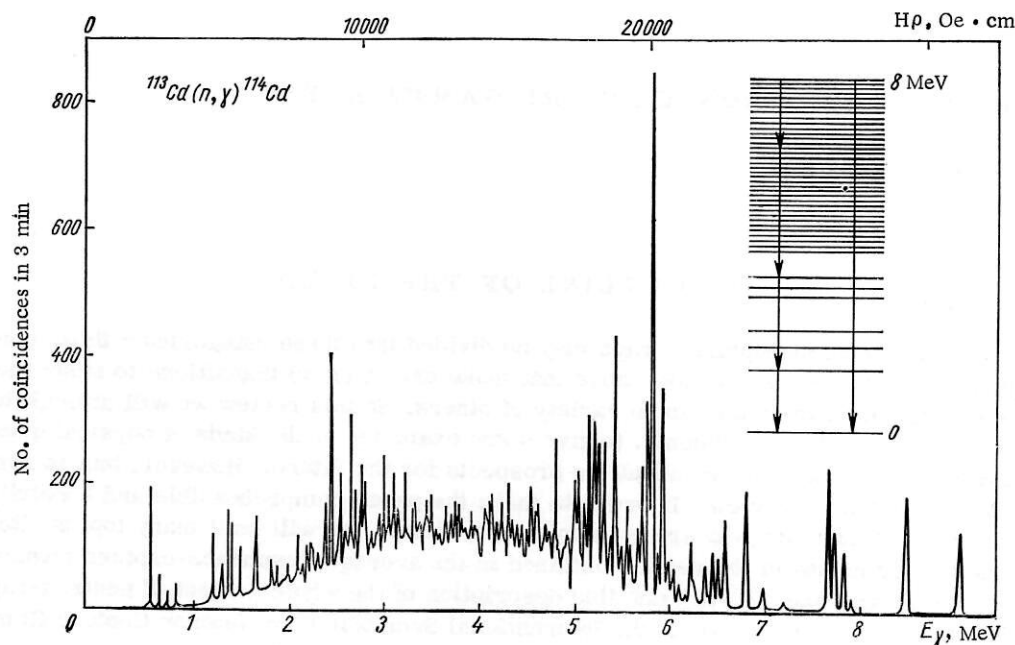


Fig. 1. Representative (n,  $\gamma$ ) spectrum for a heavy nucleus.

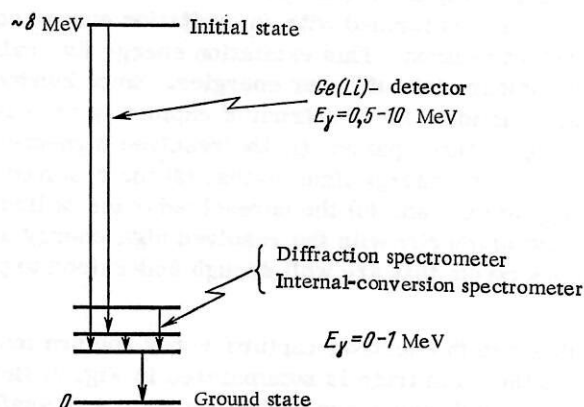


Fig. 2. The most important spectrometers used in capture  $\gamma$ -ray spectroscopy.

that may or may not be near an energy level of the nucleus. This fundamental handicap is counterbalanced by the immense intensity of neutrons available. Next in neutron energy come the various kinds of slow-neutron spectrometers (principally time-of-flight systems) that can vary the energy of the neutron. Characteristically, the  $\gamma$ -ray spectra measured with these systems are of poor technical quality and are measured over a limited range of neutron energy because the neutron intensity is inadequate; but the energy variability is a valuable asset.

At slightly higher energy (in the range 0.1-5 keV) filtered neutrons from a reactor provide a relatively intense source of neutrons that can give valuable information about the average characteristics of the  $\gamma$ -ray spectra formed by resonance neutron capture. More will be said about this approach later since it was used to obtain much of the illustrative data for this paper.

At still higher energy, the region above about 10 keV can be studied by means of electrostatic accelerators. However, the inadequate neutron fluxes achievable in this way have set rather severe limitations on the scope of the capture  $\gamma$ -ray work carried out to date, and consequently we will restrict ourselves hereafter to the much more extensive work carried out at lower neutron energies.

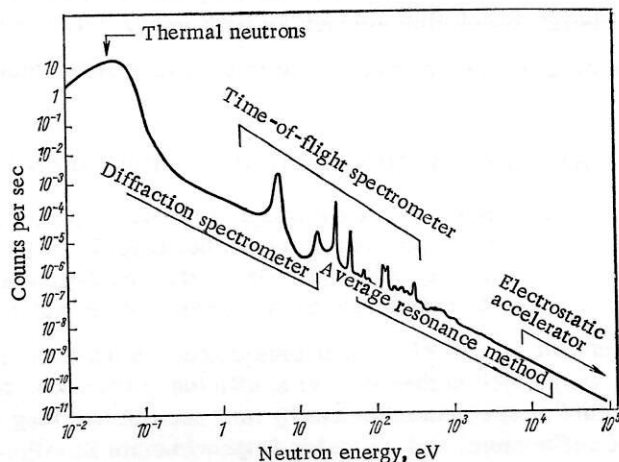


Fig. 3. Neutron sources used in neutron-capture  $\gamma$ -ray spectroscopy. Neutron sources: counts per sec per  $\gamma$ -ray line for a heavy deformed nucleus and a time-of-flight spectrometer.

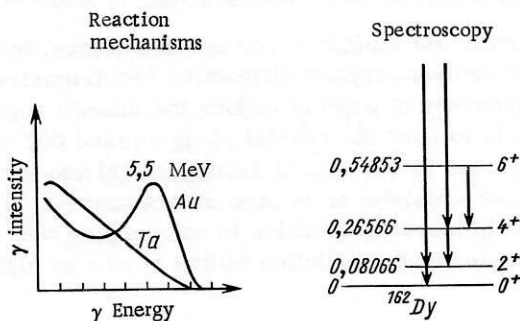


Fig. 4. Principal areas of research with neutron-capture  $\gamma$ -rays. Other uses: a) neutron-resonance spectroscopy; b) intense monoenergetic  $\gamma$ -ray sources.

And finally, "Why are neutron-capture  $\gamma$  rays interesting?" Figure 4 illustrates the principal motivations for their study. Historically first and still consuming the most scientific effort, the  $(n, \gamma)$  reaction is merely used as a way to populate low-energy nuclear states so as to obtain information about these states: thus, this area of work is very closely related to the conventional  $\gamma$ - and  $\beta$ -ray spectroscopy carried out with radioactive sources. A second important motivation for neutron-capture  $\gamma$ -ray measurements is to understand the reaction process itself. For a long time it was believed that the  $(n, \gamma)$  reaction must surely proceed by way of a compound nucleus reaction of great complexity and therefore that the capture  $\gamma$ -ray spectra are describable entirely in terms of statistical laws. However, there is a growing body of evidence that this description is not adequate for some nuclides. The third area of capture  $\gamma$ -ray spectroscopy is the use of the  $\gamma$  rays as a tool in a variety of experiments that are not primarily concerned with the  $\gamma$  rays themselves; an example is the use of the capture  $\gamma$  rays to determine the spins of neutron resonances.

A last introductory thought concerns the kind of nuclides for which the neutron capture  $\gamma$  rays are useful. The capture spectra can be measured for all stable targets and for some unstable targets, of course, but the main emphasis of the work now in progress is on a study of relatively heavy nuclides. There are two important reasons for this. First, it is only for the heavy nuclides that many resonances in a single nuclide can be studied with the available neutron sources. And second, neutron-capture  $\gamma$ -ray

spectroscopy is most competitive with other kinds of nuclear spectroscopy in the study of heavy nuclides, for which the extremely good energy resolution achievable with  $\gamma$ -ray detectors is an important asset.

With these general ideas in mind, we are now ready to turn to a more detailed discussion of several of the topics.

## II. RECENT TECHNICAL DEVELOPMENTS

Progress in the study of neutron-capture  $\gamma$  rays seems to depend on technical developments to a greater extent than in most areas of nuclear physics, perhaps because the available techniques are often just barely adequate to provide the results being sought. Thus, the development of new techniques or the refinement of those now in use is a great contribution to the growth of the science.

The technical development that is still of central importance for capture  $\gamma$ -ray spectroscopy is the Ge(Li) detector, since it has a very much higher detection efficiency than any other high-resolution  $\gamma$ -ray spectrometer. However, this kind of spectrometer has by now been in use long enough to have been developed to a very high state of refinement, and no major improvements in either the detector itself or in the associated electronics systems are visible at this time. One possibility for the future is the production of extremely large detectors. This would be a major advance for the study of resonance-capture spectra, for which higher counting rates are badly needed. Another possibility is that a new detector material with a lower band gap can be developed into a detector with a better energy resolution than Ge(Li). Although at least one material of this kind (CdTe) is being actively worked on at this time in several laboratories, the resolutions obtained to date are discouragingly poor — no better than for NaI(Tl) scintillators. Thus, one has no reason to expect large improvements in the performance of solid-state detectors soon.

In contrast to the static situation for Ge(Li)  $\gamma$ -ray spectrometers, there are continuing notable improvements in the performance of the bent-crystal diffraction spectrometer. Perhaps the most important development of this kind is the discovery of ways to reduce the mosaic spread in the diffraction crystal caused by bending. One approach is to bend the crystal along a plane that minimizes the distortion of the reflection planes, a procedure that was discovered at Leningrad [2] and is being used there and at Riso [3]. The other approach is to use thinner crystals, as is done at Argonne [4]. These developments are making the diffraction spectrometer steadily more competitive in comparison with the Ge(Li) spectrometer, and the energy at which the two systems have equal resolution widths is now as high as 2 MeV for some measurements [3].

Equally important progress is being made in internal-conversion spectrometers. Until now these systems have had such low efficiency that they have been useful principally for materials with exceptionally high capture cross sections. However, this limitation will be removed in at least two instruments now being developed. One is a system at Argonne [5] in which a superconducting solenoid is used to funnel the conversion electrons onto a solid-state detector that is some distance from the  $(n, \gamma)$  target. The effective solid angle of the detector is large for the conversion electron and small for  $\gamma$  rays. In addition to a large solid angle, the principal virtues of the system are that it records a wide range of energies simultaneously (unlike a magnetic spectrometer) and that it can be used for coincidence measurements.

A second high-sensitivity internal-conversion spectrometer is the one being developed for the new high-flux reactor at Grenoble [6]. This system, which has an  $(n, \gamma)$  target inside the reactor and a magnetic spectrograph outside, is not different in basic principle from several others, but the high flux of the reactor and a careful suppression of background are expected to result in an instrument of exceptionally high sensitivity and good energy resolution.

As will become clear later in this paper, there is an urgent need for neutron spectrometers that will allow  $\gamma$ -ray spectra to be measured for a large number of resonances in a single nuclide. The new generation of pulsed sources (especially the electron linacs) will meet a part of this need, but we suspect that they will still be inadequate for many problems, and there is no major breakthrough in sight. On the other hand, some of the information that cannot be obtained by means of  $(n, \gamma)$  measurements is now beginning to come from the inverse  $(\gamma, n)$  reaction (for example, see [7]).

Since it will be mentioned frequently in this paper, let us conclude this section on technology with an outline of an experimental development that has just reached maturity — the average-resonance method of neutron-capture  $\gamma$ -ray spectroscopy [8, 9]. The essence of the method is that the random fluctuations in



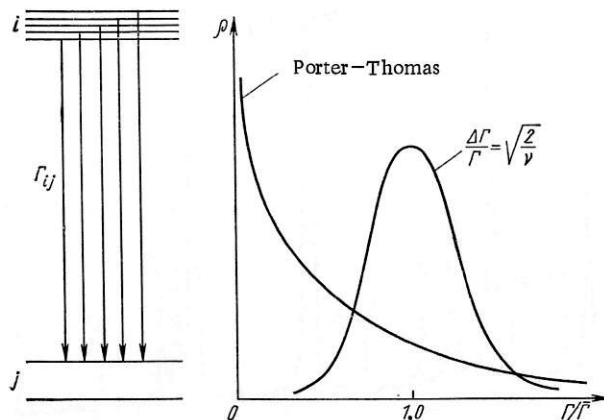


Fig. 5. The basic ideas of the average-resonance method of neutron-capture  $\gamma$ -ray spectroscopy.

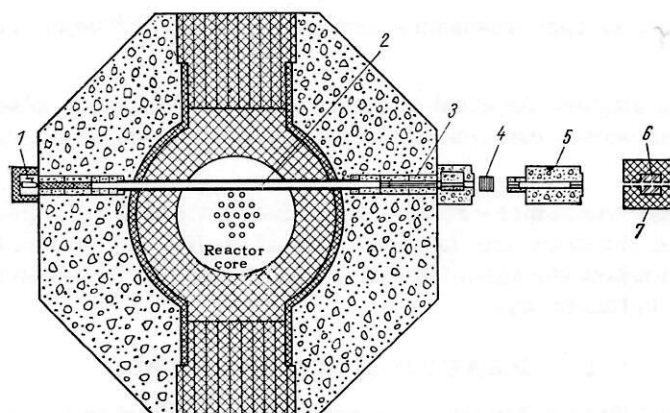


Fig. 6. An internal-target facility used for average-resonance-capture measurements [10]. 1) Source transfer mechanism; 2) sample; 3) internal collimators; 4) filters; 5) final collimator; 6) pair spectrometer; 7) Pb shield.

the intensities of high-energy radiative transitions from individual initial states are averaged out by summing the contributions from many resonances. This is done by measuring, with a Ge(Li) spectrometer, the  $\gamma$ -ray spectrum emitted by a sample that is surrounded by  $^{10}\text{B}$  and placed in a high-flux region of a nuclear reactor. The boron absorbers selectively remove low-energy neutrons, and the  $1/E$  spectrum of the incident neutron flux assures a low intensity of energetic neutrons. The combination limits the energies of the neutrons captured in the sample to a band that is broad enough to contain many neutrons but narrow enough to preserve the excellent resolution of the Ge(Li) detector and low enough in energy to restrict the capture process to s-wave and perhaps p-wave interactions.\*

The average-resonance-capture measurements at Argonne are carried out at the internal-target facility [9, 10] in the reactor CP-5, as shown in Fig. 6. Capture  $\gamma$  rays from the target are viewed by a Ge(Li) detector located outside the reactor, about 6 m from the target. A carefully designed collimation system ensures that the detector does not view the walls of the through-tube in which the target is placed. The detector is an annihilation-pair-spectrometer system consisting of a small Ge(Li) detector enclosed

\* An alternative arrangement in which a filtered neutron beam impinges on an  $(n, \gamma)$  target outside of the reactor has been described by R. C. Greenwood, R. A. Harlan, R. G. Helmer, and C. W. Reich, in *Neutron Capture Gamma-Ray Spectroscopy*, IAEA, Vienna (1969), p. 607.

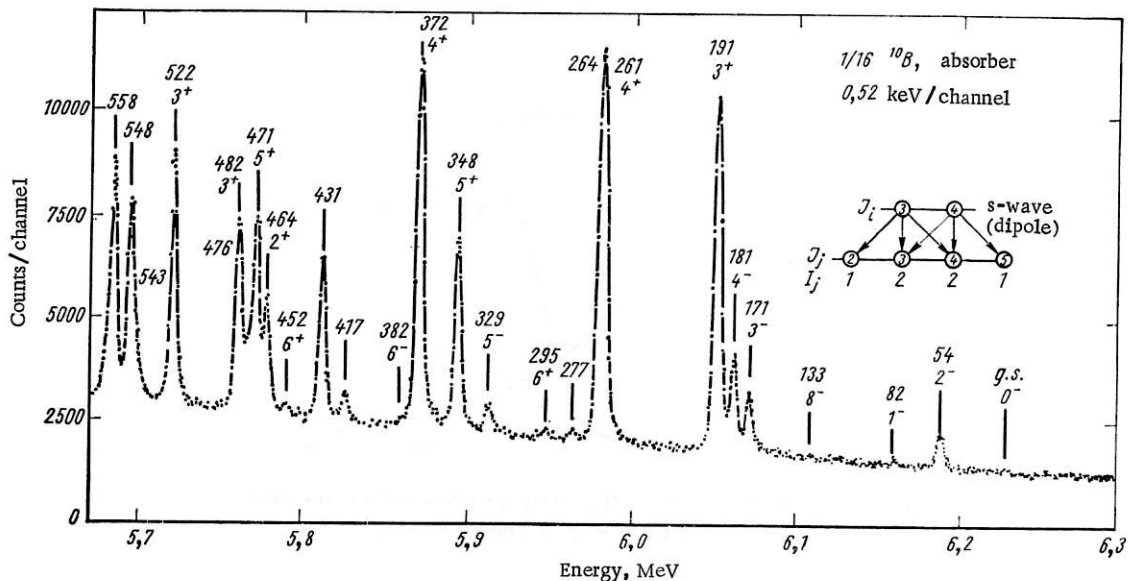


Fig. 7. The average-resonance-capture spectrum of  $^{165}\text{Ho}(n, \gamma)^{166}\text{Ho}$  [9].

in a large annulus of NaI scintillator. An event is stored in the 4096-channel pulse-height analyzer only when there is a threefold coincidence between the Ge(Li) detector and opposite quadrants of the NaI annulus.

A representative average-resonance-capture [sometimes termed  $(\bar{n}, \gamma)$ ] spectrum is shown in Fig. 7. The important features of the spectrum are its good technical quality and the fact that the  $\gamma$ -ray lines of a given kind all have approximately the same intensity. This latter feature of the spectrum will be considered in some detail later in this paper.

### III. REACTION MECHANISMS

Information about the mechanism for the  $(n, \gamma)$  process is provided by the primary transitions and, since the individual low-energy primary transitions are too weak to be observed, this in effect means high-energy transitions. As mentioned earlier, the successes of the statistical compound-nucleus model in general and of the random-matrix model of nuclear energy levels in particular suggest that, unless there is compelling evidence to the contrary, the  $\gamma$ -ray spectra formed by the capture of slow neutrons in heavy nuclei should be describable in terms of simple statistical laws that derive from the complexity of the initial state. Much of the pioneer activity in neutron-capture  $\gamma$ -ray spectroscopy since 1958 has been aimed at the testing of this idea. Let us briefly review\* a few of the recent results.

Three kinds of statistical laws are expected to apply for the high-energy radiative transitions. First, the intensity of transitions from various initial states to a single final state is a random variable with a very broad distribution. In particular, if the complexity of the initial state is complete, the relative widths  $\Gamma/\bar{\Gamma}$  for the transitions are expected to obey the well-known Porter-Thomas [13] distribution — a distribution that has the form  $x^{-1/2}e^{-x/2}$ . Second, because of the complexity of the initial state, the radiation widths are expected to be largely independent of the details of the final state. This concept has been well explained by Rosenzweig [14] in terms of a hydrodynamic model of the radiation process. And, third, the radiation widths should be uncorrelated with other widths of the initial state — in particular, uncorrelated with the neutron width or the widths for radiative transitions to other final states.

If there is some degree of simplicity in the structure of the initial state, on the other hand, there may be deviations from the statistical behavior outlined above, and these deviations or other observations may reveal something about the nature of the simple structure. The nuclear-structure concepts that have been most used in the interpretation of the capture  $\gamma$ -ray data are single-particle excitations involving the

\* Earlier reviews of the subject are those by Bollinger [11] and by Chrien [12].

TABLE 1. Summary of Experimental Evidence for the Influence of Nuclear Structure on E1 Transitions Following Neutron Capture in Heavy Nuclides with Small Level Spacings

| Phenomenon   | Experimental evidence   |
|--|---|
| 1. Energy dependence   | Giant-resonance shape for $^{56}\text{Gd}$ , $^{196}\text{Pt}$ , and others   |
| 2. Distribution of widths  | No conclusive evidence for $\nu \neq 1$   |
| 3. Interference effects from direct capture                        | Observed effect ( $^{59}\text{Co}$ , $^{238}\text{U}$ ) consistent with theory.<br>Possible influence of negative-energy resonances |
| 4. Correlation of $(n, \gamma)$ and $(d, p)$ strengths             | No conclusive evidence for correlations   |
| 5. Correlation of $(n, \gamma)$ strength and reduced neutron width | Positive correlations for $^{164}\text{Dy}$ and $^{170}\text{Tm}$   |
| 6. Correlation of radiation widths for several final states        | No conclusive evidence for correlation  |
| 7. Anomalously strong transitions                                  | No conclusive evidence for abnormal average values  |
| 8. "Bump" at $\sim 5.5$ MeV in gross spectrum for $A = 190$ -206   | Observed "bump" unexplained by statistical model for both widths and level densities  |

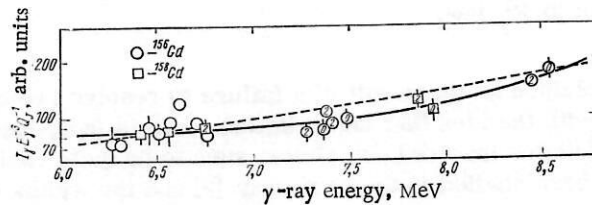


Fig. 8. Energy dependence of  $\gamma$ -ray intensity [9] for transitions in  $^{156}\text{Gd}$  and  $^{158}\text{Gd}$ . The quantity  $Q_J$  is the number (1 or 2) of transition paths that form the observed intensity. The numbers within the data points are the spins of the final states. The error bars include the effects of both experimental errors and Porter-Thomas fluctuations.

incident neutron, at the one extreme of simplicity, and collective excitation of the electric-dipole giant resonance, at the other extreme. Recently, two-particle one-hole excitations have also been discussed [15, 16]. The main aim of this section is to describe briefly the nature of the evidence for nuclear-structure effects and to give some indication of its reliability.

#### A. Statistical Behavior

The evidence for the essentially statistical behavior of the  $(n, \gamma)$  spectra is extensive. Perhaps the most striking evidence of this kind is the apparently random distribution of the widths for the high-energy radiative transitions in many nuclides. As mentioned earlier, if the initial state is completely complex, the distribution of widths is expected to obey the Porter-Thomas distribution, i.e., a  $\chi^2$  distribution with one degree of freedom. The data for many nuclides could be used to illustrate agreement with this statistical distribution, but none are better than those [17] for  $^{196}\text{Pt}$ , the first case studied with a  $\text{Ge}(\text{Li})$  detector. Other examples are listed in [12].

Another kind of evidence for the complexity of the initial state is that the average value of the radiation widths (averaged over many initial states) is largely independent of the character of the final state. This question can be studied by an average-resonance-capture measurement of the kind outlined earlier. The energy dependence for a typical nucleus is given in Fig. 8. It is seen that, within the experimental error, all but one of the data points fall along the smooth solid line drawn through the points, and this one

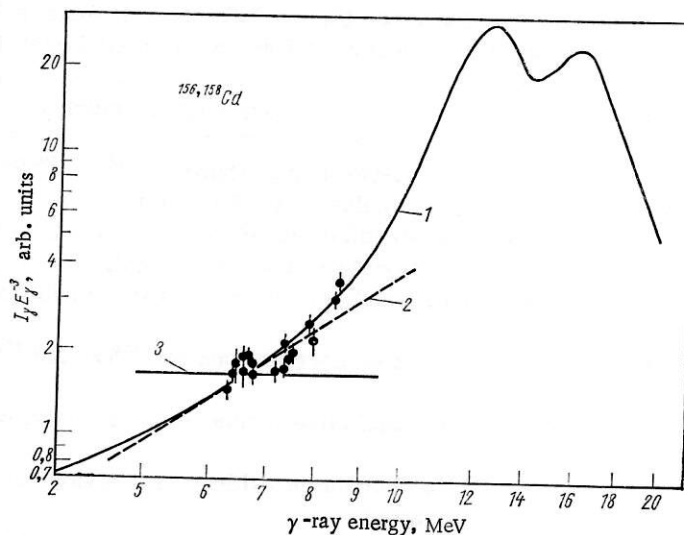


Fig. 9. Relationship of the neutron-capture  $\gamma$  rays to the E1 giant resonance. The giant-resonance curve was calculated in the way outlined in [9]. The experimental points are the same as those in Fig. 8. 1) Lorentzian shape; 2)  $E_\gamma^5$  law; 3)  $E_\gamma^3$  law.

high point can reasonably be explained as the result of a failure to resolve two closely spaced lines. Thus, the data are in good agreement with the idea that the radiation width is independent of the structure of the final state, even though the final states involved are almost sure to be quite variable in character. A large number of other nuclides have been studied in the same way [9] and the widths of almost all of them exhibit a similar smooth dependence on gamma-ray energy. An exception is  $^{170}\text{Tm}$ , for which the observed widths fluctuate more than can be explained by the statistical model. This apparent failure of the model for one nuclide is not understood.

## B. Nuclear-Structure Effects for E1 Radiation

Although the radiation widths of many nuclides satisfy rather well the predictions of the statistical model, some data seem to indicate that the structure of the initial state is simple enough to have an observable influence on the neutron-capture gamma rays. Table 1 lists the various kinds of evidence of this kind that have been discussed for E1 transitions in heavy nuclides with small level spacings at the initial state — i.e., nuclides other than those near closed shells. Let us consider several of these topics in more detail.

### 1. Giant Resonance

Some insight into the nature of the neutron-capture  $\gamma$  radiation can be obtained from the energy dependence of the radiation widths. In this respect, the most widely invoked theoretical concept is that the high-energy capture  $\gamma$  rays are formed by the same basic process as is responsible for the well-known electric-dipole giant resonance at about 13 MeV. The interpretation of the neutron-capture  $\gamma$  rays in this way involves two assumptions. Most basic is the assumption that each excited state  $E_x$  has built on it a giant resonance of the same shape as the giant resonance built on the ground state. If valid, this assumption implies that the  $\gamma$ -ray strength function  $\langle \Gamma_\gamma/D \rangle$  depends only on the  $\gamma$ -ray energy, independent of the energy of the final state. A second, less-fundamental assumption is that the photonuclear cross section is describable by a classical Lorentzian shape even at the very low energies involved in the neutron-capture  $\gamma$  radiation. The result of these two assumptions is that  $\langle \Gamma_\gamma/D \rangle$  is expected to vary much more rapidly than the  $E_\gamma^3$  dependence that results from phase-space considerations alone.\* In particular, as has been shown by Axel [18], the average width is expected to vary approximately as  $E_\gamma^5$  for  $\gamma$  rays in the neighborhood of 7 MeV.

\* An explicit relationship for the energy dependence, including the influence of quadrupole splitting, is given in [9].



The most direct evidence about the energy dependence of the radiation widths comes from the average-resonance-capture measurements. All of the measurements for many nuclides are qualitatively consistent with the energy dependence expected from the giant-resonance model, and for a few nuclides the data extend over a wide enough range to give a fairly good measure of the dependence [9]. An example is the data for  $^{156}\text{Gd}$  given in Fig. 8 and shown in relationship to the giant resonance in Fig. 9. These Gd data seem to support two conclusions: a) the overall variation in  $\Gamma_\gamma$  is about what is expected from the giant-resonance model, and b) there are significant deviations from the predictions (given by the dashed line in Fig. 8). Thus, the data provide qualitative support for the model but suggests that it is incomplete. Other nuclides for which the energy dependence is clearly stronger than  $E_\gamma^3$  are  $^{182}\text{Ta}$ ,  $^{184}\text{W}$ ,  $^{190}\text{Os}$ , and  $^{196}\text{Pt}$ .

## 2. Distribution of Partial Radiation Widths

As mentioned earlier, large fluctuations in radiation widths are observed for most nuclides, and for most of them the measured distribution of widths is consistent with the Porter-Thomas form. However, there have been reports of a failure of the Porter-Thomas distribution for some nuclides.

A quantitative analysis of the observed radiation widths is usually made by assuming that the widths obey a  $\chi^2$  distribution with  $\nu$  degrees of freedom, i.e., a distribution of the form

$$p(x) = \frac{\nu}{2} \left[ \Gamma\left(\frac{\nu}{2}\right) \right]^{-1} \left[ \frac{\nu x}{2} \right]^{(\nu/2)-1} e^{-\nu x/2}, \quad (1)$$

where  $\Gamma$  is the usual gamma function and  $x$  is the relative width. Then one uses a random-sampling technique to determine what values of  $\nu$  are consistent with the experimental sample of widths. Any set of data that is inconsistent with  $\nu = 1$  (Porter-Thomas distribution) is evidence for a failure of the concept that the initial state is infinitely complex.

A good example of the evidence for a failure of the Porter-Thomas distribution is the data obtained at the Dubna pulsed reactor by Becvar et al. [19] for transitions in  $^{142}\text{Pr}$ . Their results are shown in Fig. 10. The experimental value of  $\nu$  deduced from 27 measured widths is about 3.3. Now one must ask: Is this experimental value necessarily inconsistent with what is expected for a statistical population having  $\nu = 1$ ? This question is answered by comparing the experimental value with the distribution that is generated by computing  $\nu$  for a series of statistical samples that are randomly selected from a population for which  $\nu = 1$ . A distribution generated in this way is shown in the figure, and the experimental value is seen to be substantially larger than any of the values obtained from the mathematically generated samples. Thus, even though the experimental sample is smaller than one would wish (only three initial states and nine final states) one cannot easily escape the conclusion that the data are inconsistent with the Porter-Thomas distribution, unless there are systematic errors in the data.

Although at least five nuclides have been reported [12] as having distributions that are inconsistent with the Porter-Thomas distribution, in the opinion of the author all of these results are open to question until they have been confirmed by more extensive investigations. The reason for this doubt is that the most common experimental errors tend to bias the data in such a way as to cause the experimental value of  $\nu$  to be larger than it should be. The most important systematic errors of this kind are those that result from a failure to resolve individual final states and a failure to detect states that by chance are fed only by exceptionally weak transitions.

When the measurements are extended to high excitation energies, as is often done, errors of this kind are almost surely present. In particular, one may be confident that almost all of the data cited as evidence for  $\nu$  greater than unity contain some lines that are formed by unresolved E1 and M1 transitions. Although the M1 transition may be much weaker on the average than the E1 transition, it can have an important influence on the magnitude of the observed fluctuations in intensity. This point is illustrated in Fig. 11, where  $\chi^2$  distributions with  $\nu = 1$  and  $\nu = 2$  are compared with the distribution for the sum  $(\Gamma_{E1} + \Gamma_{M1})/\bar{\Gamma}_{E1}$  when  $\bar{\Gamma}_{E1} = 6\bar{\Gamma}_{M1}$  and both  $\Gamma_{E1}$  and  $\Gamma_{M1}$  come from a population with  $\nu = 1$ . Note that for small values of  $x$  the distribution of the sum is not unlike that for  $\nu = 2$ .

Clearly, what is needed to minimize the systematic errors caused by unresolved transitions is to restrict both the initial and final states to those that are well understood. However, the remaining sample of widths is usually so small that the statistical uncertainty is unacceptably large. Thus, there is an ur-

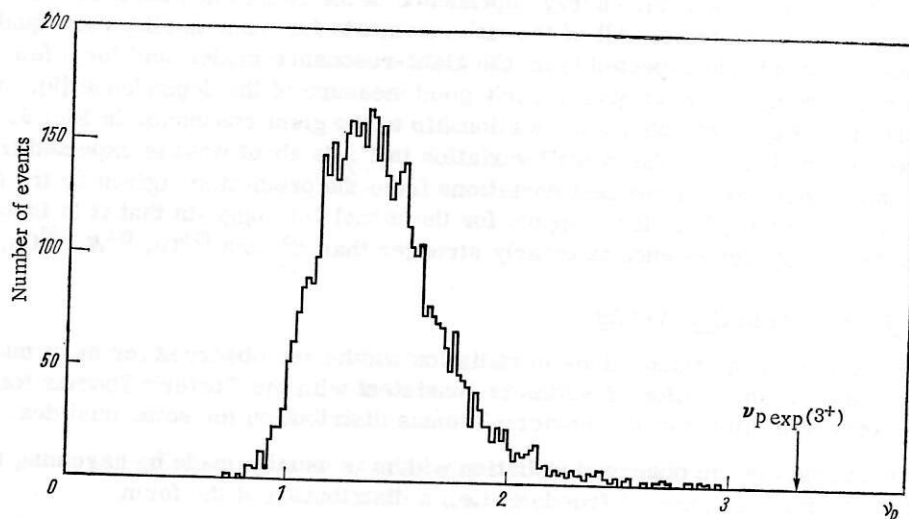


Fig. 10. Distribution of the values of  $\nu$  for samples of 27 widths that are randomly drawn from a population for which  $\nu = 1$ . The value of  $\nu$  for the corresponding experimental widths of the  $3^+$  resonances of  $^{141}\text{Pr}(n, \gamma)^{142}\text{Pr}$  is  $\nu_{p \text{ exp}} = 3.3$  [19].

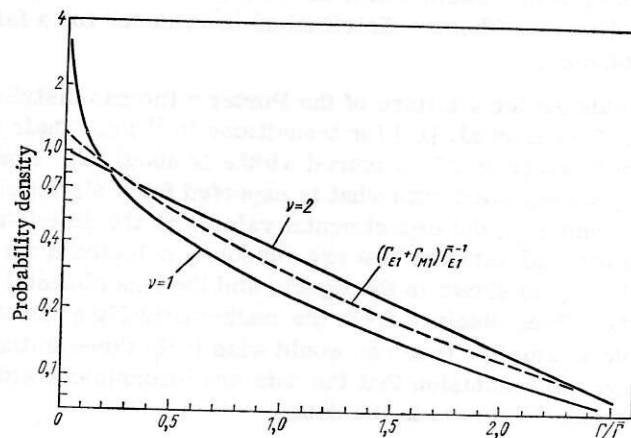


Fig. 11. Probability density functions for  $\chi^2$  distributions with 1 and 2 degrees of freedom and for the sum  $(\Gamma_{E1} + \Gamma_{M1}) / \bar{\Gamma}_{E1}$  when  $\bar{\Gamma}_{E1} = 6\bar{\Gamma}_{M1}$  and both  $\Gamma_{E1}$  and  $\Gamma_{M1}$  satisfies a  $\chi^2$  distribution with one degree of freedom. All curves are normalized to unit area.

gent need for resonance-capture measurements of much better quality and this will require much more intense sources of neutrons than have been available heretofore.

**Thermal Capture.** Although it is not related to the question of nuclear-structure effects, it is perhaps worthwhile to comment here on the distribution of intensities of lines in a thermal neutron-capture spectrum, a subject about which there seems to be some confusion. First, consider the distribution of widths from a single initial energy level to a set of final states. This distribution will satisfy the Porter-Thomas distribution, of course, if the initial level is sufficiently complex and if the average widths (averaged over many initial states) of all final states are the same. But what if the initial state is at an energy at which many resonances of the same spin contribute to the capture cross section, as is often the case for thermal-neutron capture? Does the presence of many contributing resonances tend to average out the fluctuations in intensity? A little thought shows that it does not — the distribution still obeys the Porter-Thomas distribution (if all of the initial states have the same spin). The reason is that the amplitudes (rather than the

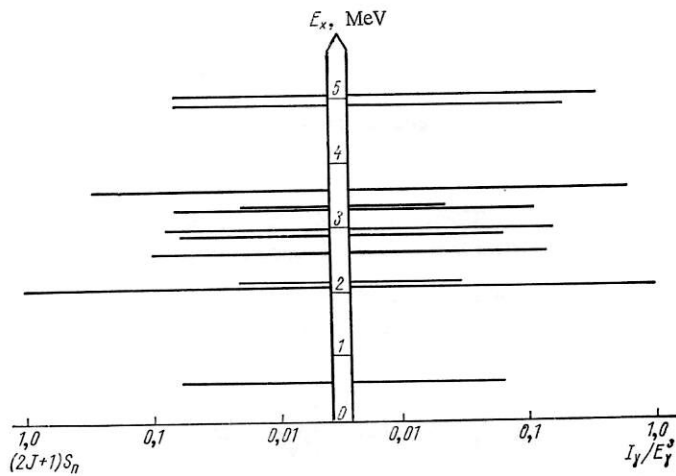


Fig. 12. Comparison of strength of (d, p) and (n, γ) transitions to levels in  $^{43}\text{Ca}$  [23].

cross sections) associated with the various resonances add to form the intensity of interest, and since each of these components is normally distributed, the sum is also normally distributed. Thus, the distribution of width is governed by the Porter-Thomas distribution. This expectation is consistent with the experimental results reported many years ago by Bartholomew [20] when one takes into account the complications involved in the interpretation of the spectra, including the possibility of contributions by two initial spin states.

### 3. Correlations with (d, p) Cross Sections and Neutron Widths

The usual analysis of the distribution of radiation widths is a relatively insensitive way in which to search for departures from statistical behavior because the analysis does not make use of a nuclear model and information from other experiments. In contrast, the search for correlations between the radiation widths and other widths commonly makes use of the formalism of Lane and Lynn [21], who describe the amplitude for the capture process in terms of three components - an "internal" compound-nucleus resonance part, an "external" or "channel" resonance part, and, a "hard-sphere" part. The internal resonance contribution exhibits the familiar statistical behavior that is insensitive to nuclear structure, whereas both channel resonance and hard-sphere capture depend on the single-particle character of the final state. This formalism provides a useful stimulus and guide in the search for nonstatistical effects whether or not there is reason to believe that the theory is accurately applicable in any given case.

**Thermal Capture.** The cross sections for both hard-sphere capture and channel resonance capture are proportional to the neutron width of the final capture, it may be looked for by comparing the  $\gamma$  ray intensities with the intensities of the  $l = 1$  component of (d, p) transitions to the same final states. Strong correlations between the (n, γ) and (d, p) strengths have been found for many nuclides with  $A < 70$ , as summarized by Groshev et al. [22]. Excellent examples are the recent data reported by Arnell et al. [23] for the Ca isotopes, one of which is shown in Fig. 12. Such data indicate that the off-resonance cross sections for some of the medium-weight nuclides are dominated by either hard-sphere capture or channel resonance capture. However, the thermal-capture data alone do not indicate which of the two processes is dominant, and for nuclides with large level spacings it has not yet been feasible to study channel resonance capture by measuring refined  $\gamma$  spectra for many resonances.

For heavy nuclides, nearby resonances usually contribute heavily to the thermal-capture cross section and the observed fluctuations in the intensities of the observed  $\gamma$  rays have the random amplitudes expected for the internal resonance-capture component. These fluctuations thoroughly obscure the possible components that depend on the character of the final states.

**Resonance Capture.** The transition amplitude associated with resonance capture may be written\* as

\* This equation is based on the result of Lane and Lynn [21], but the energy dependence  $f(E_\gamma)$  is introduced to allow for the influence of the giant resonance. In practice, it is unimportant whether the  $E_\gamma^3$  dependence associated with the first term is accurate, in view of the huge fluctuations in  $A_j^2$  and  $\Gamma_n^0$ .

$$\Gamma_{\gamma ij}^{1/2} = \{ A_j \Gamma_{ni}^{01/2} E_\gamma^{3/2} + R_{ij}^{1/2} [f(E_\gamma)]^{1/2} \}, \quad (2)$$

where  $\Gamma_{\gamma ij}^{1/2}$  is the amplitude for a radiative transition from an initial state  $i$  to a final state  $j$ ,  $A_j^2$  is proportional to the neutron width of the final state,  $\Gamma_{ni}^0$  is the reduced neutron width of the initial state,  $R_{ij}^{1/2}$  is a random variable with a normal distribution, and  $f(E_\gamma)$  is a function of  $\gamma$ -ray energy. The first term results from channel capture and the second term from internal compound-nucleus capture.

The relationship of Eq. (2) to the resonance-capture data is most easily appreciated by considering the average widths under two alternative conditions. First, the average width of transitions from many initial states to a single final state is

$$\frac{\langle \Gamma_{\gamma i} \rangle_i}{f(E_\gamma)} = A_j^2 \langle \Gamma_{ni}^0 \rangle \frac{E_\gamma^3}{f(E_\gamma)} + \langle R_i \rangle_i. \quad (3)$$

Second, the average width of transitions from a single initial state to many final states is

$$\frac{\langle \Gamma_{\gamma i} \rangle_i}{f(E_\gamma)} = \langle A_j^2 \rangle_i \Gamma_{ni}^0 \frac{E_\gamma^3}{f(E_\gamma)} + \langle R_i \rangle_i. \quad (4)$$

The quantity  $A_j^2$  is accurately proportional to  $(2J_j + 1)S_j$ , where  $S_j$  is the spectroscopic factor for the  $l = 1$  component, but in practice this quantity is often unknown for heavy nuclides, and one must be satisfied to use instead the measured  $(d, p)$  cross section  $\sigma_{dp}$  at an arbitrary angle.

Most efforts to demonstrate the presence of channel capture have been devoted to heavy nuclei, since only for them is it technically feasible to measure the  $\gamma$ -ray spectra of many resonances. No evidence for the nonrandom component is found for a large fraction of the nuclides studied. However, for the reactions  $^{169}\text{Tm}(n, \gamma)^{170}\text{Tm}$  and  $^{163}\text{Dy}(n, \gamma)^{164}\text{Dy}$  the Brookhaven group have reported [24-26] convincing evidence that the widths of radiative transitions to low-energy final states depend on the reduced neutron widths of the initial states. The relationship of this observation to the channel capture theory is not entirely clear since, according to the theory, a correlation with the neutron widths necessarily implies that there is a correlation with the  $(d, p)$  strength, and this correlation is not observed [26, 27] for  $^{170}\text{Tm}$  and  $^{164}\text{Dy}$ .

There are several reports of statistically significant correlations between the  $(d, p)$  cross sections and radiation widths observed in resonance capture. One of these is for  $^{165}\text{Ho}(n, \gamma)^{166}\text{Ho}$ , which was studied by means of the Brookhaven fast chopper. Chrien [12] reported that the coefficient of correlation between the  $(n, \gamma)$  strength (presumably meaning  $\Gamma_\gamma / E_\gamma^3$ ) and the  $(d, p)$  cross section is +0.48 and that there is only a 2.2% chance that such a high value could occur by chance if the widths are uncorrelated. This result can be sensitively checked by means of an average-resonance-capture measurement. According to Eq. (3), a plot of  $\langle \Gamma_{\gamma i} \rangle_i / f(E_\gamma)$  vs  $\sigma_{dp} E_\gamma^3 / f(E_\gamma)$  should form a linear curve with a positive slope and an intercept at  $\langle R_i \rangle$ . The average widths  $\langle \Gamma_{\gamma i} \rangle_i$ , measured at the internal target facility at Argonne are plotted in this way in Fig. 13. First consider the illustration in the upper left, which gives  $\Gamma_\gamma / E_\gamma^3$  vs  $\sigma_{dp}$ . Here there seems to be a strong correlation between the two quantities, and indeed a straight-line fit of the data would be roughly the same as the dashed line, which corresponds to the previously reported correlation coefficient  $\rho = 0.48$ . Moreover, the data are inconsistent with  $\rho = 0$ , since the observed deviations of the points from a horizontal line would occur by chance less than 0.1% of the time.

In the above example the function  $f(E_\gamma)$  was set equal to  $E_\gamma^3$ , as is usually done in correlation studies. However, the gadolinium data mentioned earlier show that  $f(E_\gamma)$  may vary much more rapidly than  $E_\gamma^3$ . The giant-resonance model probably describes the energy dependence in some average sense, but it certainly would not be unexpected if in a short range of energy the radiation widths deviate from the giant-resonance shape for reasons that are unrelated to the single-particle character of the final state. Thus, in order to make a sensitive test for  $(n, \gamma) - (d, p)$  correlation one should use the energy dependence that is most appropriate for the data being analyzed. For the  $^{166}\text{Ho}$  data [9], the energy dependence in the range involved ( $E_x = 190-600$  keV) is well described by  $f(E_\gamma) = E_\gamma^{7.2}$ . The correlation plot for this energy dependence is given at the lower left of the figure. Here the evidence for correlation has largely disappeared, as is shown quantitatively by the small value  $\chi^2 = 10.4$  for a horizontal-line fit of the data.



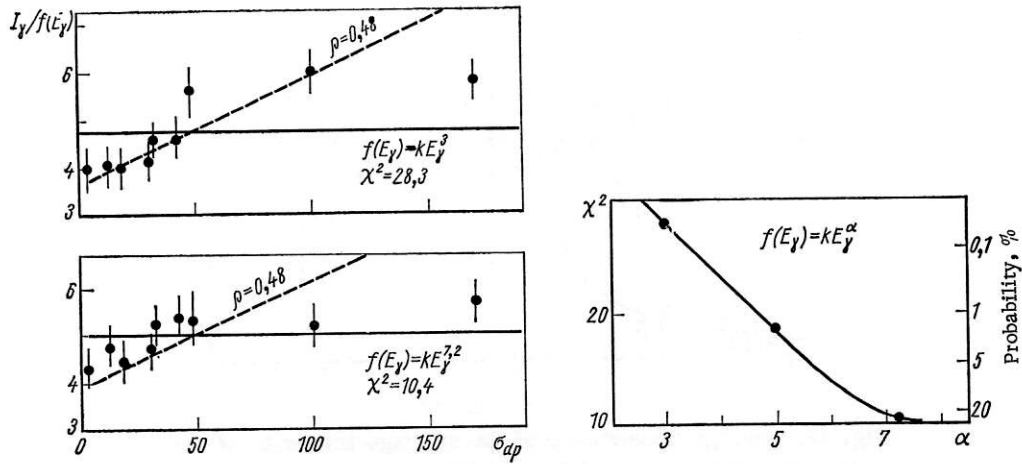


Fig. 13. Search for a dependence of the average radiation width  $\langle \Gamma_{\gamma j} \rangle$  on the (d, p) cross section  $\sigma_{dp}$ . The  $^{165}\text{Ho}(n, \gamma)^{166}\text{Ho}$  widths are from [9] and the (d, p) intensities from Struble et al. [28]. (n, r) - (d, p) correlation;  $r_{ij}^{1/2} = (A_i r_{ni}^{01/2} +$

$$i_{ij}^{1/2})^{1/2} (E_{\gamma}); \quad \frac{\langle \Gamma_{\gamma j} \rangle}{I(E_{\gamma})} = \sigma_{dp} + < R_j >; \quad I(E_{\gamma}) = k E_{\gamma}^{\alpha}.$$

A similar treatment of the  $(\bar{n}, \gamma)$  data [9] for  $^{166}\text{Er}(n, \gamma)^{167}\text{Er}$ , a second reaction cited [12] as evidence for (d, p) correlations, shows that the correlation is much weaker than was inferred previously from the spectra measured at individual resonances [12]. The new result is  $\rho = 0.28_{-0.37}^{+0.12}$ , which again is consistent with  $\rho = 0$ .

The data of Fig. 13 show that the use of an inaccurate energy dependence can cause a serious bias in a correlation analysis. This effect is expected to be present for many heavy nuclides, since for many the (d, p) transition strength tends to diminish rapidly with increasing excitation energy. Thus, the author concludes that there is no convincing experimental evidence that the widths of radiative transitions in heavy nuclei (other than closed-shell nuclei) depend on the single-particle character of the final state.

#### 4. Summary of Data on E1 Transitions in Heavy Nuclei

Let us return now to Table 1, which outlines the kinds of data that have been cited as evidence for the influence of nuclear structure on the E1 transitions in heavy nuclides. In our opinion, only the giant-resonance behavior and the correlation between neutron and radiation widths are well established in the sense that only for them are there no known questions about the data or contradictions with other reliable data. It is also true that the much discussed [15] "bump" in the unresolved spectra of nuclides with  $A = 190-206$  has not been explainable without recourse to a nuclear-structure model of the radiation process, and the only reason for doubting this interpretation is that the resolved transitions for the same nuclides are so ordinary in behavior.

The scarcity of unquestionable information about the influence of nuclear structure on the high-energy E1 transitions is an accurate reflection of the difficulty of the experiments required to obtain such information. The urgent need for more powerful experimental methods is apparent.

#### C. M1 Radiation

Years of study of thermal-neutron-capture  $\gamma$  rays have shown that magnetic dipole (M1) transitions are an order of magnitude weaker than electric-dipole transitions in most nuclides. As a result, the M1 transitions are hard to study and we have relatively little detailed understanding of their behavior. This void is being rapidly filled, however, by the results of new techniques of measurement - in particular, by average-resonance-capture and by threshold photoneutron measurements.

A complication of the absolute values of M1 transitions was reported [11] earlier and recent results [9] are in generally good agreement with the conclusion that the average widths of M1 transitions in the energy range 6.5 to 8.5 MeV are roughly

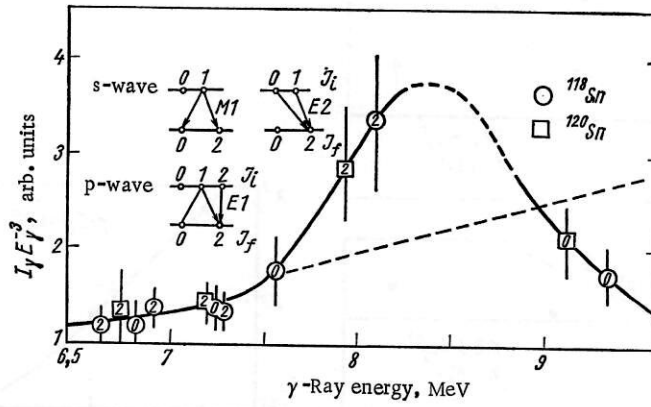


Fig. 14. Energy dependence of the average intensity of radiative transitions to positive-parity states fed by  $^{117}\text{Sn}(n, \gamma)^{118}\text{Sn}$  and  $^{119}\text{Sn}(n, \gamma)^{120}\text{Sn}$  [29]. The error bars include the effects of both experimental error and Porter-Thomas fluctuations. The numbers within the data points are the spins of the final states.

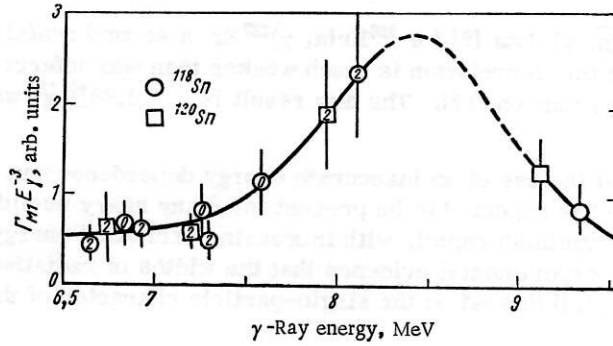


Fig. 15. Energy dependence of the average widths of the M1 component of high-energy transitions in  $^{118}\text{Sn}$  and  $^{120}\text{Sn}$  [29].

$$\Gamma_{M1} \approx 0.002 D_i E_\gamma^3$$

for most nuclides. Here  $\Gamma_{M1}$  is in eV and both  $D$  and  $E_\gamma$  are in MeV.

A recurring question about the M1 radiation has been whether or not there is evidence for an M1 giant resonance in the energy range 5-10 MeV. One indication for such a resonance has been the reports of anomalously strong M1 transitions in a few nuclides such as  $^{117}\text{Sn}$  and  $^{138}\text{Ba}$ . The significance of such data can now be studied systematically by means of average-resonance-capture measurements. The results [29] for the reactions  $^{117}\text{Sn}(n, \gamma)^{118}\text{Sn}$  and  $^{119}\text{Sn}(n, \gamma)^{120}\text{Sn}$  are given in Fig. 14, where the intensities of  $\gamma$ -ray lines that contain M1 components are plotted as a function of  $\gamma$ -ray energy. The data points are seen to fall along a resonance-like curve, but one must ask whether the apparent resonance could be accounted for by chance fluctuations of intensity. The answer is that the solid curve drawn through the data is not very meaningful, since the energy dependence represented by the dashed curve is not totally inconsistent with the data. However, at the very least one may conclude that there is an exceptionally large variation in the  $\gamma$ -ray intensity over the energy range 6.5-9 MeV. Also, the apparent peak in the  $(\bar{n}, \gamma)$  intensity is similar to one reported [30] recently in the cross section for the inverse reaction  $^{118}\text{Sn}(\gamma, n)^{117}\text{Sn}$ .

The interpretation of the observed intensity shown in Fig. 14 is complicated by the fact that it consists of three components, as shown at the top left of the figure. On the basis of the results for other nuclides [9]

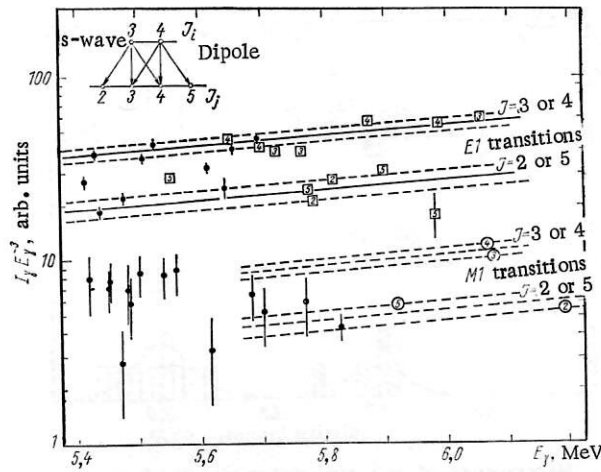


Fig. 16. Plot of  $\bar{I}_\gamma E_\gamma^3$  vs  $E_\gamma$  for  $^{165}\text{Ho}(n, \gamma)^{166}\text{Ho}$  [9]. The numbers within some of the points are the J values reported by Motz et al. [33]. The error bars associated with the points are rms errors of measurement; where no error is given, the error is smaller than the size of the point. The dashed lines associated with each solid line indicated the expected rms scatter caused by Porter-Thomas fluctuations;  $\square$ ) positive polarity;  $\circ$ ) negative polarity;  $\bullet$ ) unknown.

the E2 contribution may be neglected, and the magnitude of the p-wave component can be deduced from the observed shape of the  $\gamma$ -ray line, as discussed elsewhere [9]. The corrected intensity attributable to M1 radiation is given in Fig. 15. Here the resonance-like shape is even more apparent. Such a resonance could result from a "spin-flip" transition between the  $h_{11/2}$ ,  $h_{9/2}$  subshells of the shell-model orbital [31]. The width of the resonance is somewhat smaller than that calculated by Shapiro and Emery [32] for heavier, more deformed, nuclei. Unfortunately, the analysis of the data has not yet proceeded far enough to indicate whether or not the absolute values of the transitions in the peak of the curve in Fig. 16 are abnormally large.

#### IV. THE SPECTROSCOPY OF LOW-ENERGY STATES

As mentioned earlier, the largest effort in neutron-capture  $\gamma$ -ray spectroscopy is devoted to the study of low-energy nuclear states. A variety of techniques and neutron sources are used, but since a discussion of all of these would extend this paper intolerably, we have chosen to restrict the discussion to a single example — a study of the states of  $^{166}\text{Ho}$  carried out most recently by means of an average-resonance-capture measurement [9].

A part of one of the  $(\bar{n}, \gamma)$  spectra for  $^{165}\text{Ho}(n, \gamma)^{166}\text{Ho}$  has already been shown in Fig. 7. Since the  $\gamma$ -ray lines in the spectrum are formed by transitions directly to low-energy final states, the excitation energies  $E_x$  of these final states are simply equal to the neutron-binding energy minus the energies of the observed lines. The main advantage of the  $(\bar{n}, \gamma)$  method is that the spins and parities of the low-energy states may also be determined from the observed  $\gamma$  rays.

The simple ideas involved in the determination of spins and parities from the  $(\bar{n}, \gamma)$  data are summarized by the diagram at the upper left of Fig. 16. The basic assumption is that the average widths of a given class of radiative transitions is a smooth function of  $\gamma$ -ray energy and that the widths of transitions between individual states satisfy the Porter-Thomas distribution. Then the average intensity of the line associated with a given final state is approximately proportional to the number of ways  $Q_J$  in which the state is reached and to the strength function  $\langle \Gamma_\gamma / D \rangle$  for the kind of radiation involved. In practice, only s-wave capture followed by either E1 or M1 radiation has significant intensities for a large number of nuclides (including  $^{166}\text{Ho}$ ), and consequently there are only four combinations of  $\Gamma_\gamma / D$  and  $Q_J$ . Thus, in a plot of  $\Gamma_\gamma / E_\gamma^3$  vs  $E_\gamma$  all points are expected to fall along one of four lines, if the measurement involves

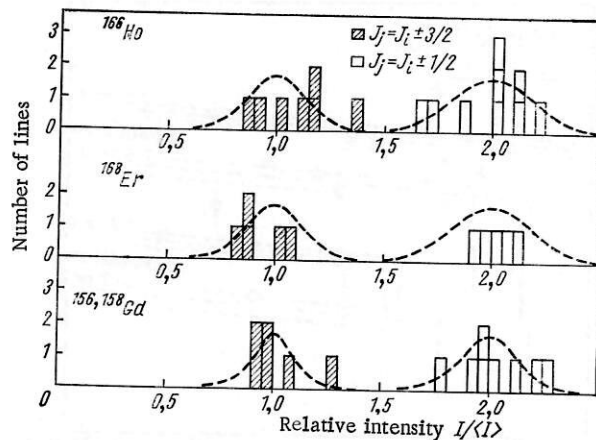


Fig. 17. Histogram of relative intensities of average-resonance-capture transitions [9].

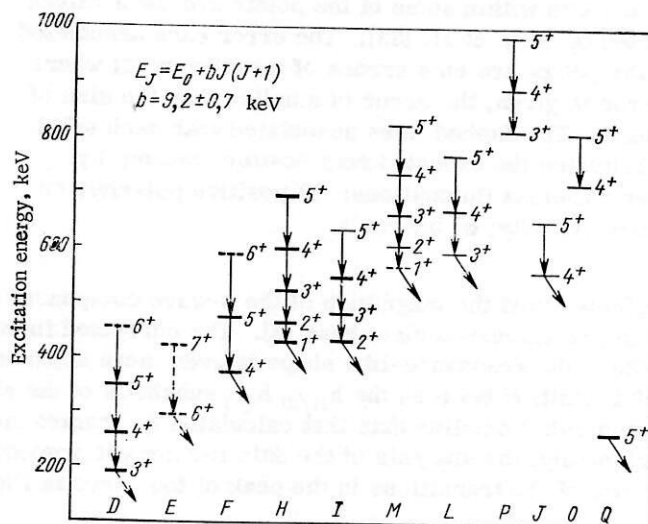


Fig. 18. Positive-parity bands of  $^{166}\text{Ho}$  [9]. The states represented by heavy lines were reported by Motz et al. [33]. The connecting vertical lines represent low-energy  $\gamma$  rays that have been reported [33] and the diagonal lines identify states from which relatively strong transitions are observed. The letters at the bottom are arbitrary labels for the bands.

enough initial states to average out most of the random intensity fluctuations. Figure 16 shows that the expected behavior is indeed satisfied by the well-resolved lines of  $^{166}\text{Ho}$  — the lines for  $E_x < 600$  keV. Notice that the intensities for E1 and M1 lines are well separated and that the two classes of spin states are also easily distinguishable. Hence, the parities of the final states and narrow limits on the spins can be determined immediately from the observed intensities.

An appealing way in which to display the basic validity of the  $(\bar{n}, \gamma)$  method of spin assignment is to plot a histogram of the relative intensity  $I_\gamma/\bar{I}_\gamma$  for states of previously known spin, where  $\bar{I}_\gamma$  is taken from a smooth curve drawn through the data points in a plot of  $I_\gamma$  vs  $E_\gamma$ . The results of such a histogram are given in Fig. 17, where the intensities of states with  $J_j = J_0 \pm 3/2$  are seen to be well separated from those with  $J_j = J_0 \pm 1/2$ , as expected from the model.

The  $(\bar{n}, \gamma)$  measurements for  $^{166}\text{Ho}$  reveal a very large number of low-energy nuclear states for which the parity is known with certainty and the spin is known to be either 2 or 5, on the one hand, or 3 or 4, on



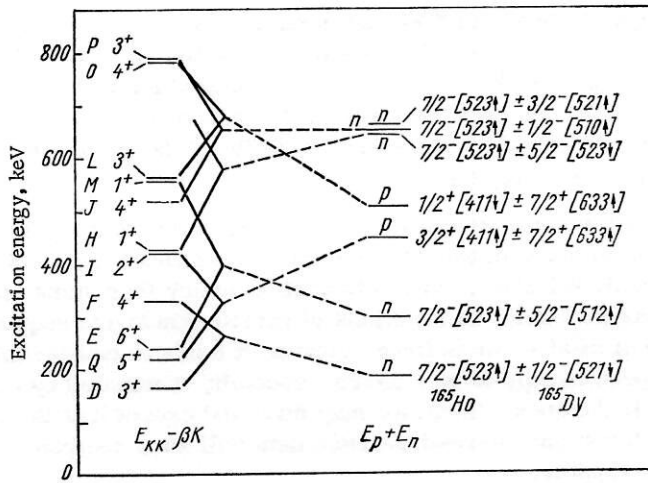


Fig. 19. Comparison of observed and predicted positive-parity bands in  $^{166}\text{Ho}$  [9]. Band labels and K values of the experimental bands are given on the left. Suggested configurations of the intrinsic states in  $^{165}\text{Ho}$  and  $^{165}\text{Dy}$  that combine to form states in  $^{166}\text{Ho}$  are given on the right. The letters n and p identify states that result from neutron-excited and proton-excited states, respectively. Each connected pair of bands satisfies the Gallagher-Moszkowski coupling rules.

the other. Since the characteristics of the  $(\bar{n}, \gamma)$  method lead one to expect that all positive-parity states with  $E_x < 850$  keV have been detected in the measurements, the  $^{166}\text{Ho}$  data offer an opportunity for an unusually extensive description of the rotational band structure of nuclear levels in a heavy deformed nucleus. The result obtained for the positive-parity states is shown in Fig. 18. Each band was identified by searching for positive-parity states whose energies  $E_J$  forms a sequence with energies at

$$E_J = E_0 + bJ(J+1), \quad (5)$$

(where  $E_0$  and  $b$  are constants) and whose  $\gamma$ -ray intensities are consistent with what is required by the spin  $J$ . In this way all 31 of the positive-parity states detected below 850 keV can be fitted into rotational bands that have reasonable characteristics, and this suggests strongly that all of the states with  $J = 2, 3, 4$ , or 5 have been detected and correctly identified. The negative-parity data are less complete, because the M1 transitions that feed them are sometimes obscured by the much stronger E1 transitions to positive-parity states. Altogether, the measurements reveal 16 rotational bands (7 of which have been identified previously) giving one of the largest number of bands yet reported for any single nuclide. It should be emphasized that it is the completeness of the  $(\bar{n}, \gamma)$  data and the fact that the measurements provide unambiguous information about states (rather than about transitions between states) that make the band-structure analysis convincing.

Additional information about the rotational bands of  $^{166}\text{Ho}$  can be obtained by checking to see whether the  $\gamma$  rays that should connect the adjacent members of each band were observed in the low-energy  $\gamma$ -ray spectra reported by Motz et al. [33]. In all cases, there is a  $\gamma$  ray of the appropriate energy. Moreover, strong transitions are observed to emanate from most of the band heads, as would be expected. This consistency between the energies of the states observed in our work and the low-energy  $\gamma$ -ray lines reported previously tends to confirm the validity of the band structure.

The states in  $^{166}\text{Ho}$  may be interpreted in terms of a model in which the odd neutron and odd proton are independently coupled to a  $^{164}\text{Dy}$  core. Then the intrinsic states of the odd particles may be determined from the known states of  $^{165}\text{Ho}$  and  $^{165}\text{Dy}$ , and these intrinsic states may be combined to form rotational bands in  $^{166}\text{Ho}$ ; the energies of the band heads are (in rough approximation) equal to the sum  $E_p + E_n$  of the energies of the proton-excited and neutron-excited intrinsic states, and the spins  $K$  of the band heads are related to the spins  $\Omega_p$  and  $\Omega_n$  of the intrinsic states by  $K = |\Omega_p \pm \Omega_n|$ .

The observed positive-parity bands of  $^{166}\text{Ho}$  are compared in Fig. 19 with the first-order predictions of the model. Here the sum  $E_p + E_n$  of energies of intrinsic states in  $^{165}\text{Ho}$  and  $^{165}\text{Dy}$  and the corresponding quantity  $E_{KK} - \beta K$  for the observed  $^{166}\text{Ho}$  bands were calculated from the experimental data, where  $E_{KK}$  is the energy of the band head. The qualitative agreement between the observed bands in  $^{166}\text{Ho}$  and the theoretical expectations seems to establish the overall validity of the model and again tends to confirm the reliability of the band-structure analysis.

A characteristic feature of the above result for  $^{166}\text{Ho}$  is that the capture  $\gamma$ -ray measurements provide data about a larger number of states than can be detected and identified in any other way in a heavy deformed nucleus, but they provide relatively little information (other than spins and parities) about the structure of these states. Charged-particle reactions of various kinds are required to complete the picture. This is a healthy state of affairs, we believe, because it tends to counterbalance the strong tendency for neutron-capture  $\gamma$ -ray spectroscopy to be a narrow specialty dominated by emphasis on specialized and demanding experimental techniques. Thus, we may hope and expect that the obvious advantage that is gained from a union of the neutron and charged-particle data will keep neutron-capture  $\gamma$ -ray spectroscopy in the mainstream of nuclear physics.

#### LITERATURE CITED

1. Neutron Capture Gamma-Ray Spectroscopy, International Atomic Energy Agency, Vienna (1969).
2. O. I. Sumbaev and A. I. Smirnov, Nucl. Instrum. Meth., **22**, 125 (1963).
3. H. R. Koch et al., in: Neutron Capture Gamma-Ray Spectroscopy, IAEA, Vienna (1969), p. 65.
4. R. K. Smither and D. J. Buss, in: Neutron Capture Gamma-Ray Spectroscopy, IAEA, Vienna (1969), p. 55.
5. S. B. Burson, in: Argonne National Laboratory Report ANL-7436 (1968), p. 3.
6. T. von Egidy, in: Neutron Capture Gamma-Ray Spectroscopy, IAEA, Vienna (1969), p. 127.
7. C. D. Bowman, B. L. Berman, and H. E. Jackson, Phys. Rev., **178**, 1827 (1969).
8. L. M. Bollinger and G. E. Thomas, Phys. Rev. Letters, **18**, 1143 (1967).
9. L. M. Bollinger and G. E. Thomas, Phys. Rev., **C2**, 1951 (1970).
10. G. E. Thomas, D. E. Blatchley, and L. M. Bollinger, Nucl. Instr. Methods, **56**, 325 (1967).
11. L. M. Bollinger, in: Nuclear Structure, International Atomic Energy Agency, Vienna (1968), p. 317.
12. R. E. Chrien, in: Neutron Capture Gamma-Ray Spectroscopy, IAEA, Vienna (1969), p. 627.
13. C. E. Porter and R. G. Thomas, Phys. Rev., **104**, 483 (1956).
14. N. Rosenzweig, Nucl. Phys., **A118**, 650 (1968).
15. G. A. Bartholomew, in: Neutron Capture Gamma-Ray Spectroscopy, IAEA, Vienna (1969), p. 553.
16. K. Rimawi et al., Phys. Rev. Letters, **23**, 1041 (1969).
17. H. E. Jackson et al., Phys. Rev. Letters, **17**, 656 (1966).
18. P. Axel, Phys. Rev., **126**, 671 (1962).
19. F. Becvar et al., in: Neutron Capture Gamma-Ray Spectroscopy, IAEA, Vienna (1969), p. 651.
20. G. A. Bartholomew, in: Proceedings of the Conference on Electromagnetic Lifetimes and Properties of Nuclear States, Gatlinburg, Tenn., 1961. National Academy of Sciences Report NAS-NRC 974 (1962), p. 209.
21. A. M. Lane and J. E. Lynn, Nucl. Phys., **17**, 563 (1960).
22. L. V. Groshev and A. M. Demidov, Yadernaya Fiz., **4**, 785 (1966).
23. S. E. Arnell, R. Hardell, O. Skeppstedt, and E. Wallander, in: Neutron Capture Gamma-Ray Spectroscopy, IAEA, Vienna (1969), p. 231.
24. M. Beer et al., Phys. Rev. Letters, **20**, 340 (1967).
25. R. E. Chrien, in a short contribution following [11]; also see Fig. 8 of [11].
26. S. F. Mughabghab, R. E. Chrien, and O. A. Wasson, Brookhaven National Laboratory Report BNL-14 982 (1970).
27. L. M. Bollinger and G. E. Thomas, Bull. Am. Phys. Soc., **13**, 722 (1968).
28. G. L. Struble, J. Kern, and R. K. Sheline, Phys. Rev., **137**, 772 (1965).
29. L. M. Bollinger and G. E. Thomas, to be published.
30. E. J. Winhold, E. M. Bowey, D. B. Gayther, and B. H. Patrick, Harwell Preprint (1970).
31. D. M. Brink, in: Argonne National Laboratory Report ANL-6797 (1963), p. 194.
32. C. S. Shapiro and G. T. Emery, Phys. Rev. Letters, **23**, 244 (1969).
33. H. T. Motz et al., Phys. Rev., **155**, 1265 (1967).